Effects of *Arctostaphylos uva-ursi* Extract as Green Corrosion Inhibitor for Cu10Ni Alloy in 1 M HNO₃

Y.M.Abdallah[1,], Hala M. Hassan[2], K.Shalabi[3] and A.S. Fouda[3]*

[1] Faculty of Oral and Dental medicine, Delta University for Science and Technology, Gamsa, El-Mansoura, Egypt.
[2] Textile Technology Department, Industrial Education College, Beni-Suef University, Egypt and Chemistry Department, Faculty of Science, Jazan University, KSA
[3] Department of Chemistry, Faculty of Science, El-Mansoura University, El-Mansoura-35516, Egypt, Fax: +2 0502246254
[*]E-mail: dr.ymostafa80@yahoo.com

The corrosion inhibition of Cu10Ni alloy by Arctostaphylos uva-ursi extract (AUUE) in 1 M HNO₃ has been investigated by potentiodynamic polarization, electrochemical impedance spectroscopy (EIS), electrochemical frequency modulation (EFM) and scanning electron microscope (SEM) techniques. Potentiodynamic polarization indicated that AUUE acted as mixed type inhibitor but mainly cathodic. The calculated adsorption thermodynamic parameters indicated that the adsorption was a spontaneous, exothermic process accompanied by an increase in entropy and obey Langmuir adsorption. The inhibition efficiency increases with increasing the concentration of the inhibitor and decreases with increasing the temperature. The SEM results showed the formation of a protective film on the alloy surface in the presence of AUUE. The results obtained from different electrochemical techniques were in good agreement.

1. INTRODUCTION

Copper is a metal that has a wide range of applications due to its outstanding properties. This metal can be easily alloyed with other elements to form a great class of materials known as copper base alloys. These alloys have a long history of service in marine environments and saline water systems. The importance of corrosion studies is two fields. The first is economic, including the reduction of material losses resulting from the wasting away or sudden failure of piping, tanks, metal

components of machines, ships, hulls, marine and structures [1]. The second is conservation, applied primarily to metal resources, the world's supply of which is limited, and the wastage of which includes corresponding losses of energy and water resources accompanying the production and fabrication of metal structures [2]. Almost all organic molecules containing heteroatoms such as nitrogen, sulphur, phosphorous, and oxygen show significant inhibition efficiency. Despite these promising findings about possible corrosion inhibitors, most of these substances are not only expensive but also toxic thus causing pollution problems. Hence, these deficiencies have prompted the search for their replacement. Inhibitors containing double or triple bonds play an important role in facilitating the adsorption of these compounds onto metal surfaces [3]. A bond can be formed between the electron pair and/or the π-electron cloud of the donor atoms and the metal surface, thereby reducing corrosive attack in an acidic medium. Although many of these compounds have high inhibition efficiencies, several have undesirable side effects, even in very small concentrations, due to their toxicity to humans, deleterious environmental effects, and its high-cost [4]. Plant extract is low-cost and environmental safe, so the main advantages of using plant extracts as corrosion inhibitor are economic and safe environment. Up till now, many plant extracts have been used as effective corrosion inhibitors for Cu10Ni alloy in acidic media, such as: Tobacco extract in 3.5%NaCl solution [5] , Nypa Fruticans Wurmb [6] , Mango, Cashew, Passion fruit, Orange, Khillah seeds, African bush pepper, Neem leaves and papaya [7] , Non–chromates [8] , Cassia Acutifolia, Ziziphus Spinachristi, Lupinus Termis, Brassica Nigra and Trigon Ella foenum-graecum [9], Ficus Carica and Olive leaves [10], Solanum Melongena L. leaf extract [11], were protected against corrosion using some plant extracts.

The inhibition performance of plant extract is normally ascribed to the presence of complex organic species, including tannins, alkaloids and nitrogen bases, carbohydrates and proteins as well as hydrolysis products in their composition. These organic compounds usually contain polar functions with nitrogen, sulfur, or oxygen atoms and have triple or conjugated double bonds or aromatic rings in their molecular structures, which are the major adsorption centers. Arctostaphylos uva-ursi is a plant species of the genus Arctostaphylos (manzanita). Its common names include kinnikinnick and pinemat manzanita, and it is one of several related species referred to as bearberry [12]. The distribution of Arctostaphylos uva-ursi is circumpolar, and it is widespread in northern latitudes, but confined to high altitudes further south. Bearberry has historically been used for medicinal purposes. It contains the glycoside Arbutin, which has antimicrobial properties and acts as a mild diuretic. It has been used for urinary tract complaints, including cystitis and urolithiasis. An infusion may be made by soaking the leaves in ethanol and then diluting with water [13]. In the 19th century before the introduction of sulfa drugs and modern antibiotics, it was among the few herbal drugs with antibacterial properties, but some constituents, such as the hydroquinones arehepatotoxic, and in cases of urinary tract infections, more pertinent treatment options are recommended [14].

The objective of this study was to investigate the inhibitory effect of Arctostaphylos uva-ursi extract (AUUE) as a green corrosion inhibitor for Cu10Ni alloy in 1 M HNO_3 using various electrochemical techniques. Surface morphology was also studied and discussed.

2. EXPERIMENTAL METHODS

2.1. Materials and solutions

The working electrode was made from Cu10Ni rod. The rod was mounted into a glass tube and fixed by araldite leaving a circle surface geometry of 1 cm diameter to contact the test solution. Prior to each experiment, the working electrode was polished with a different grades of emery paper up to 1200 grade, rinsed with acetone and finally with doubly distilled water. The auxiliary electrode was platinum wire, while a saturated calomel electrode (SCE) connected to conventional electrolytic cell of capacity 100 ml. The aggressive solution used was prepared by dilution of analytical reagent grade 70% HNO_3 with bidistilled water. The stock solution (2000 ppm) of AUUE was used to prepare the desired concentrations by dilution with bidistilled water. The concentration range of AUUE used was 50-500 ppm.

2.2. Preparation of plant extracts

Fresh aerial parts of Arctostaphylos uva-ursi leaves were collected from Mansoura University garden, Mansoura, Egypt in spring (April 2013). Then identified by Botany Department, Faculty of Science, Mansoura University, Egypt. The Plant materials of Arctostaphylos uva-ursi leaves were shade dried at room temperature for 13 days. The shade dried plant materials were crushed to make fine powder. The powdered materials (100 g each) were soaked in 250 ml of methanol for 5 days and then subjected to repeated extraction with 25×30 ml until exhaustion of plant materials. The extracts obtained were then concentrated under reduced pressure using rotary evaporator at temperature below 55°C. The methanol evaporated to give solid extract that was prepared for application as corrosion inhibitor.

The plant contains arbutin, methylarbutin, a bitter principle, ursolic acid, tannic acid, gallic acid, some essential oil and resin, hydroquinones (mainly arbutin, up to 17%), tannins (up to 15%), phenolic glycosides and flavonoids. [15].

2.3. Electrochemical measurements

Electrochemical measurements were performed using a typical three-compartment glass cell consisting of the Cu10Ni alloy specimen as working electrode (1 cm^2), saturated calomel electrode (SCE) as a reference electrode, and a platinum foil (1 cm^2) as a counter electrode. The reference electrode was connected to a Luggin capillary and the tip of the Luggin capillary is made very close to the surface of the working electrode to minimize IR drop. All the measurements were done in solutions open to atmosphere under unstirred conditions. All potential values were reported versus SCE. Prior to each experiment, the electrode was abraded with successive different grades of emery paper, degreased with acetone, also washed with bidistilled water, and finally dried.

Tafel polarization curves were obtained by changing the electrode potential automatically from (-0.8 to 1 V vs. SCE) at open circuit potential with a scan rate of 1 mVs^{-1}. Stern-Geary method [16],

used for the determination of corrosion current is performed by extrapolation of anodic and cathodic Tafel lines to a point which gives (log i_{corr}) and the corresponding corrosion potential (E_{corr}) for inhibitor free acid and for each concentration of inhibitor. Then (i_{corr}) was used for calculation of inhibition efficiency (IE %) and surface coverage (θ) as in equation 1:

$$IE\% = \theta \times 100 = \left[1 - \frac{i_{corr\,(inh)}}{i_{corr\,(free)}}\right] \times 100 \qquad (1)$$

where $i_{corr(free)}$ and $i_{corr(inh)}$ are the corrosion current densities in the absence and presence of inhibitor, respectively .

Impedance measurements were carried out in frequency range (2×10^4 Hz to 8×10^{-2} Hz) with amplitude of 10 mV peak-to-peak using AC signals at open circuit potential. The experimental impedance was analyzed and interpreted based on the equivalent circuit. The main parameters deduced from the analysis of Nyquist diagram are the charge transfer resistance R_{ct} (diameter of high-frequency loop) and the double layer capacity C_{dl}.

The inhibition efficiencies and the surface coverage (θ) obtained from the impedance measurements are calculated from equation 2:

$$IE\% = \theta \times 100 = \left[1 - \left(\frac{R_{ct}^{\circ}}{R_{ct}}\right)\right] \times 100 \qquad (2)$$

where R°_{ct} and R_{ct} are the charge transfer resistance in the absence and presence of inhibitor, respectively.

Electrochemical frequency modulation, EFM, was carried out using two frequencies 2 and 5 Hz. The base frequency was 0.1 Hz, so the waveform repeats after 1 s. The higher frequency must be at least two times the lower one. The higher frequency must also be sufficiently slow that the charging of the double layer does not contribute to the current response. Often, 10 Hz is a reasonable limit. The Intermodulation spectra contain current responses assigned for harmonical and intermodulation current peaks. The large peaks were used to calculate the corrosion current density (i_{corr}), the Tafel slopes (β_a and β_c) and the causality factors CF-2 & CF-3 [17]. The electrode potential was allowed to stabilize 30 min before starting the measurements. All the experiments were conducted at 25°C .

All electrochemical measurements were performed using Gamry Instrument (PCI4/750) Potentiostat/Galvanostat/ZRA. This includes a Gamry framework system based on the ESA 400. Gamry applications include DC105 software for potentiodynamic polarization, EIS 300 software for electrochemical impedance spectroscopy, and EFM 140 software for electrochemical frequency modulation measurements via computer for collecting data. Echem Analyst 6.03 software was used for plotting, graphing, and fitting data. To test the reliability and reproducibility of the measurements, duplicate experiments were performed in each case at the same conditions

2.4. Surface examination

The surface films were formed on the Cu10Ni specimens by immersing them in AUUE solutions for a period of 24 h. After the immersion period, the specimens were taken out, dried and the nature of the film formed on the surface of the metal specimen was analyzed by SEM techniques.

Examination of Cu10Ni surface after 24 h exposure to the 1 M HNO$_3$ solution without and with AUUE was carried out by JEOL JSM-6510 Scanning Electron Microscope.

3. RESULTS AND DISCUSSION

3.1. Potentiodynamic Polarization

Polarization curves were shown in Figure (1) for Cu10Ni alloy in 1 M HNO$_3$ in the absence and presence of different concentrations of AUUE at 25ºC. It is clear that both anodic metal dissolution and cathodic H$_2$ reduction reactions were inhibited when AUUE was added to 1 M HNO$_3$ and this inhibition was more pronounced with increasing extract concentrations. Tafel lines are shifted to more negative and more positive potentials with respect to the blank curve by increasing the concentration of the investigated inhibitors. This behavior indicates that AUUE act as mixed-type inhibitors [18]. The values of corrosion potential, (E$_{corr}$), corrosion current density (i$_{corr}$), Tafel slopes (β$_a$, β$_c$), corrosion rate (CR) and inhibition efficiency obtained from these measurements are listed in Table (1). It is clear from this Table that the corrosion current density decreases with increasing the concentration of the investigated extract. Moreover the small negative shift of corrosion potential indicates that AUUE is arranged as a mixed type inhibitor, with predominant cathodic effectiveness. The lower values of (i$_{corr}$) in the presence of investigated extract without causing significant changes in (E$_{corr}$) values suggest that AUUE is mainly mixed-type inhibitors [19, 20].

The decrease in the corrosion current density and the increase in the inhibition efficiency may be attributed to the adsorption of the investigated extract on the alloy surface.
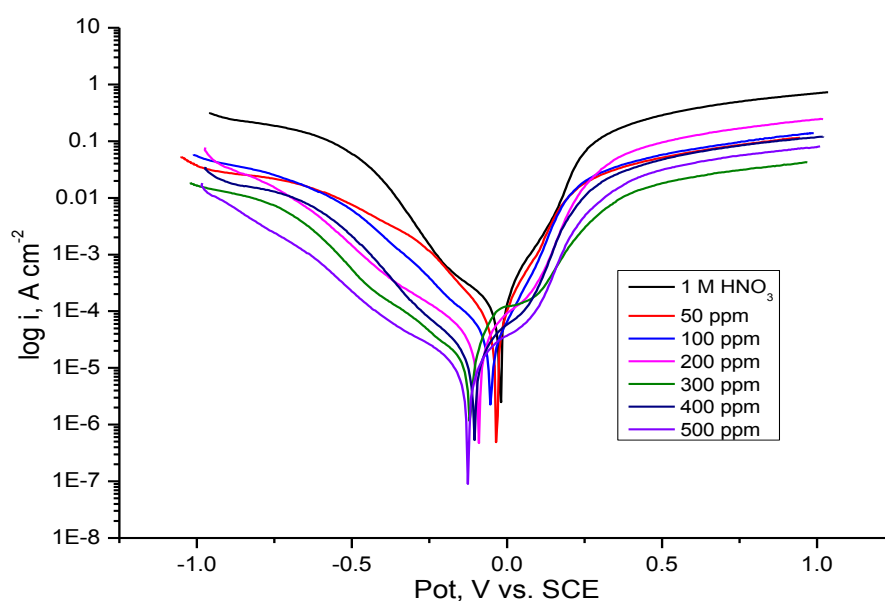

Figure 1. Potentiodynamic polarization curves for Cu10Ni alloy in 1 M HNO$_3$ in the absence and presence of different concentrations of AUUE at 25 °C

Table 1. Polarization parameters for Cu10Ni alloy in 1 M HNO₃ in the absence and presence of various concentrations of the AUUE at 25 °C.

Concentration, ppm.	-E_{corr}, mV vs SCE	i_{corr}, µA cm^{-2}	β_c, mV dec^{-1}	β_a, mV dec^{-1}	Corrosion Rate, mpy	Θ	%IE
1 M HNO₃	21	68.0	162	90	31.07	---	---
50	34	35.3	170	91	16.14	0.481	48.1
100	51	32.2	190	107	14.72	0.526	52.6
200	91	25.2	193	151	11.51	0.629	62.9
300	119	18.1	188	184	8.27	0.734	73.4
400	105	13.3	182	154	6.07	0.804	80.4
500	126	8.6	171	186	3.95	0.873	87.3

3.2. Electrochemical impedance spectroscopy (EIS) measurements

Figure (2) shows impedance plots for Cu10Ni alloy in 1 M HNO₃ solution without and with different concentrations of the investigated extract. The impedance spectra consists of a Nyquist semicircle type without appearance of diffusive contribution to the total impedance (Z) indicating that the corrosion proceeds mainly under charge-transfer control and the presence of inhibitor do not alter the mechanism of corrosion reaction.
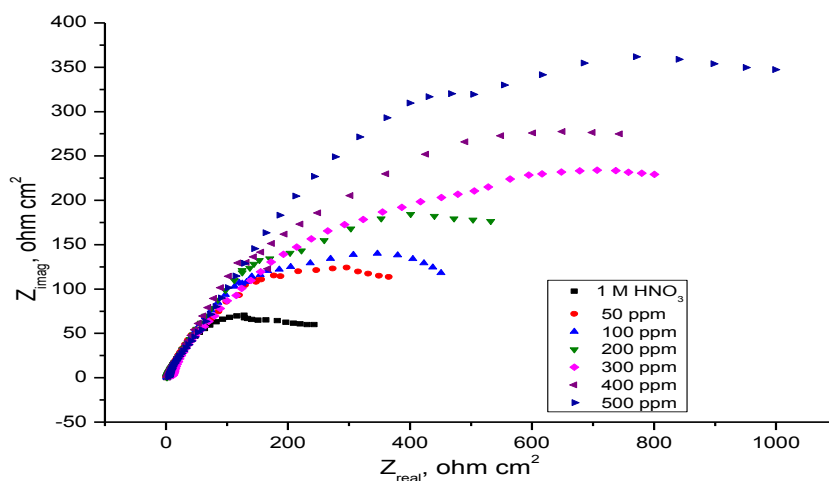

Figure 2. The Nyquist plots for Cu10Ni alloy in 1 M HNO₃ solution in the absence and presence of different concentrations of AUUE at 25 °C

It is found that the obtained Nyquist plots are not perfect semicircle due to frequency dispersion and this behavior can be attributed to roughness and inhomogeneity's of the electrode surface [21, 22].

When there is non-ideal frequency response, it is common practice to use distributed circuit elements in an equivalent circuit. The most widely employed is the constant phase element (CPE). In general a CPE is used in a model in place of a capacitor to compensate for inhomogeneity in the

system [23]. It was found that the diameters of the semicircle increases with increasing the concentration of the investigated extract. This indicates that the polarization resistance of the oxide layer increases with increasing the concentration of AUUE and the depressed capacitive semicircle are often referred to the surface roughness and inhomogeneity, since this capacitive semicircle is correlated with dielectric properties and thickness of the barrier oxide film [24]. The data revealed that, each impedance diagram consists of a large capacitive loop with low frequencies dispersion (inductive arc). This inductive arc is generally attributed to anodic adsorbed intermediates controlling the anodic process [25-27]. By following this, inductive arc was disregarded.

The electrical equivalent circuit model shown in Figure (3) was used to analyze the obtained impedance data. The model consists of the solution resistance (R_s), the charge-transfer resistance of the interfacial corrosion reaction (R_{ct}) and the constant phase angle element (CPE). The value of frequency power (n) of CPE can be assumed to correspond to capacitive behavior. However, excellent fit with this model was obtained with our experimental data. The admittance of CPE is described as:

$$Y_{CPE} = Y_o (j\omega)^n \tag{3}$$

where (j) is the imaginary root, (ω) the angular frequency, (Y_o) the magnitude and (n) is the exponential term [28].
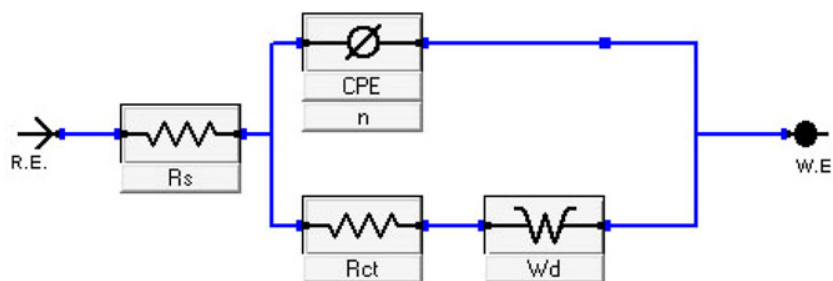

Figure 3. Equivalent circuit model for the corrosion of Cu10Ni displaying Warburg impedance.

A long Warburg diffusion tail was observed at low frequency values. The tails are inclined at an angle of 45° to the real-axis at the very low frequencies; A diffusion controlled process is therefore exists. Studies reported in the literature [29] showed that the diffusion process is controlled by diffusion of dissolved oxygen from the bulk solution to the electrode surface and the Warburg impedance, which is observed in the low frequency regions, is ascribed to diffusion of oxygen to the alloy surface. This diffusion tail still appears, even in presence of high concentrations of the investigated extract. This means that the corrosion behavior of alloy in the absence as well as in the presence of AUUE is influenced by mass transport.

Also, Bode plots for the Cu10Ni alloy in 1 M HNO_3 solution are shown in Figure (4). In which the high frequency limit corresponding to the electrolyte resistance (ohmic resistance) R_Ω, while the low frequency represents the sum of ($R_\Omega + R_{ct}$), where R_{ct} is in the first approximation determined by both electrolytic conductance of the oxide film and the polarization resistance of the dissolution and repassivation process. At both low and high frequency limits, the phase angle between the current and potential (θ), assumes a value of about 0°, corresponding to the resistive behavior of R_Ω and ($R_\Omega + R_{ct}$).

The main parameters deduced from the analysis of Nyquist diagram are:

- The resistance of charge transfer R_{ct} (diameter of high frequency loop)
- The capacity of double layer C_{dl} which is defined as :

$$C_{dl} = \frac{1}{2\pi R_{ct} f_{max}}$$ (4)

where (f_{max}) is the maximum frequency at which the (Z_{imag}) of the impedance is a maximum. Since the electrochemical theory assumed that ($1/R_{ct}$) is directly proportional to the capacity of double layer (C_{dl}), the inhibition efficiency (%IE) of the inhibitor for Cu10Ni alloy in 1 M HNO$_3$ solution was calculated from (R_{ct}) values obtained from impedance data at different AUUE concentration the following equation:

$$\% IE = \left(1 - \frac{R_{ct}^{\circ}}{R_{ct}}\right) \times 100$$ (5)

where (R°_{ct}) and (R_{ct}) are the charge transfer resistance in the absence and Presence of investigated extract, respectively.
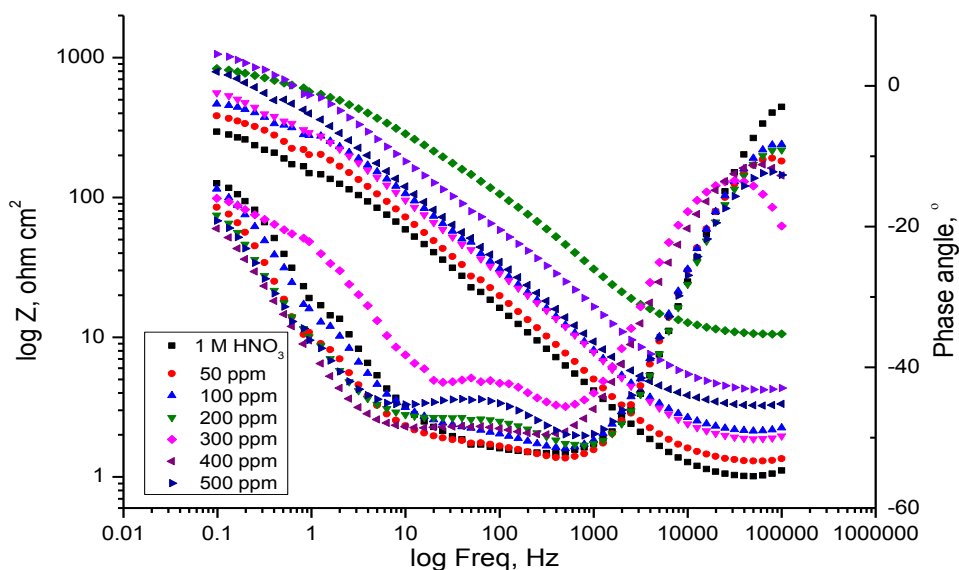

Figure 4. Bode plots recorded for Cu10Ni alloy in 1 M HNO$_3$ without and with various concentrations of AUUE at 25˚C

From the impedance data given in Table (2), we can conclude that the value of (R_{ct}) increases with the increase in the concentration of the investigated extract and this indicates that the formation of a protective film on the alloy surface by the adsorption and an increase in the corrosion inhibition efficiency in acidic solution. While the value of (C_{dl}) decreases with increasing the concentrations of extract in comparison with that of blank solution (1 M HNO$_3$), as a result from the replacement of water molecules by inhibitor molecules which lead to decrease in local dielectric constant and/or an increase in the thickness of the electric double layer formed on Cu10Ni alloy [30,31].

Table 2. Electrochemical kinetic parameters obtained by EIS technique for Cu10Ni in 1 M HNO$_3$ solutions containing various concentrations of AUUE at 25°C

Concentration, ppm.	R_{ct}, Ωcm^2	Y_o	N	C_{dl}, x10^4 $\mu F\ cm^{-2}$	W, $\mu\Omega^{-1}cm^{-2}\ s^{1/2}$	θ	% IE
1 M HNO3	190.4	8.49E-4	0.666	443	1.41E-2	---	---
50	338.2	7.97E-4	0.650	3.94	8.53E-3	0.437	43.7
100	387.1	7.22E-4	0.645	3.58	7.03E-3	0.508	50.8
200	464.1	6.61E-4	0.621	3.22	4.88E-3	0.590	59.0
300	641.7	5.84E-4	0.612	3.14	4.30E-3	0.703	70.3
400	777.7	5.38E-4	0.600	3.01	3.37E-3	0.755	75.5
500	1023.0	4.01E-4	0.592	2.17	2.85E-3	0.814	81.4

3.3. Electrochemical frequency modulation (EFM) method

The EFM is a nondestructive corrosion measurement technique that can directly give values of the corrosion current without prior knowledge of Tafel constants. Like EIS, it is a small signal AC technique. Unlike EIS, however, two sine waves (at different frequencies) are applied to the cell simultaneously. Intermodulation spectra obtained from EFM measurements in absence and presence of different concentrations of AUUE are presented in Figures (5), (6) as examples of Cu10Ni alloy in 1 M HNO$_3$ solutions at 25°C, 45°C respectively . Each spectrum is a current response as a function of frequency. The two large peaks are the response to the 2 Hz and 5 Hz excitation frequencies. The harmonic and intermodulation peaks are clearly visible software package to calculate the corrosion current and Tafel constants The calculated corrosion kinetic parameters at different concentrations of AUUE in 1 M HNO$_3$ at 25°C and 45°C (i$_{corr}$, β_a, β_c, CF-2, CF-3 and % IE) are given in Table (3). The corrosion current densities decrease by increasing the concentration of inhibitors and hence, inhibition efficiency increases. The causality factors are very close to theoretical values which according to EFM theory should guarantee the validity of Tafel slopes and corrosion current densities [32]. The standard values for CF-2 and CF-3 are 2.0 and 3.0, respectively. The deviation of causality factors from their ideal values might due to the perturbation amplitude was too small or the resolution of the frequency spectrum is not high enough also another possible explanation that the inhibitor is not performing very well. The inhibition efficiencies IE$_{EFM}$ % increase by increasing the studied extract concentrations and was calculated as follows:

$$IE\ \%_{EFM} = \left(1 - \frac{i_{corr}}{i^{o}_{corr}}\right) \times 100 \tag{6}$$

where (i$^{o}_{corr}$) and (i$_{corr}$) are corrosion current densities in the absence and presence of AUUE, respectively.
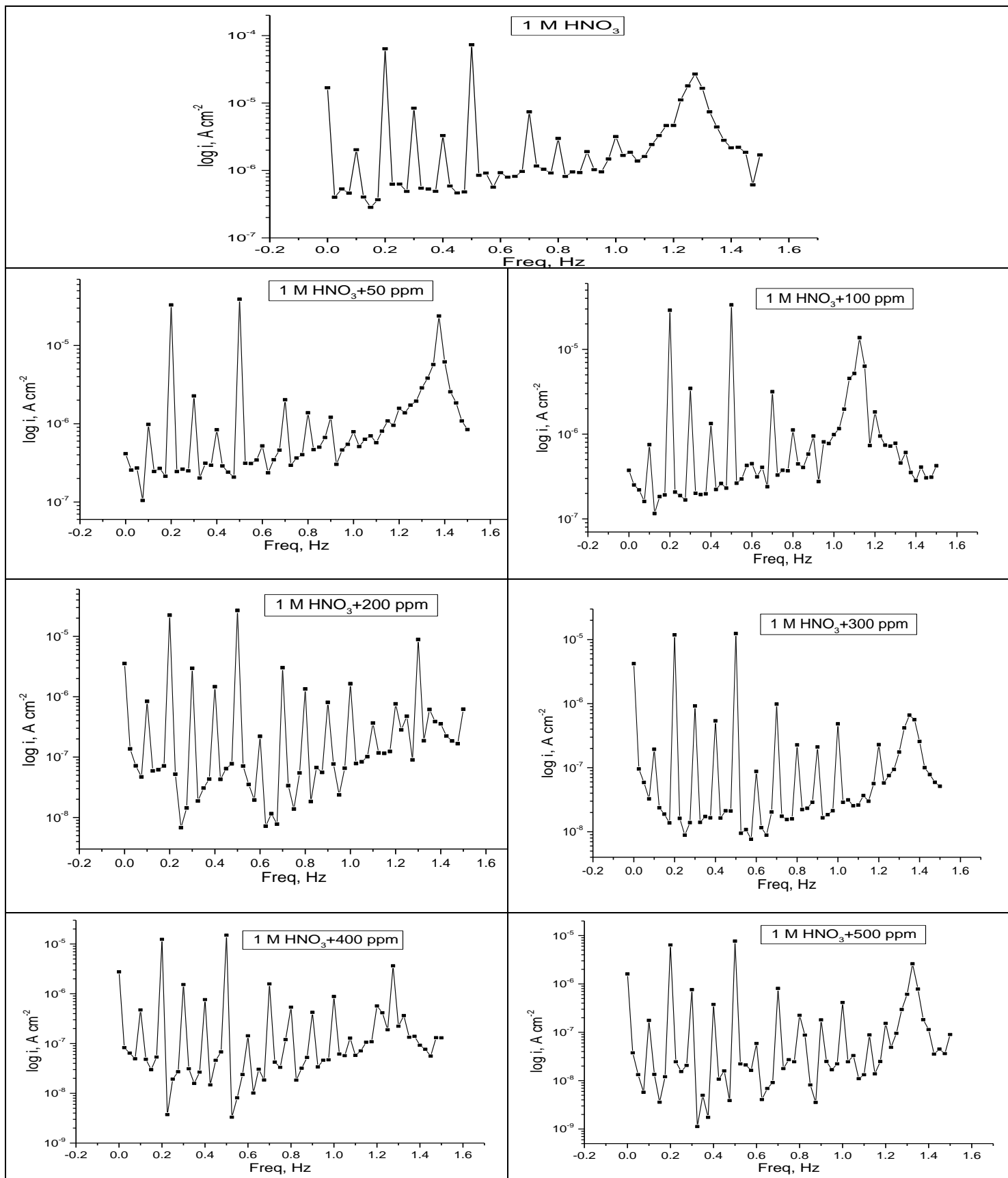
Figure 5. Intermodulation spectrum for Cu10Ni alloy in 1 M HNO_3 solutions without and with various concentrations of AUUE at 25ºC.
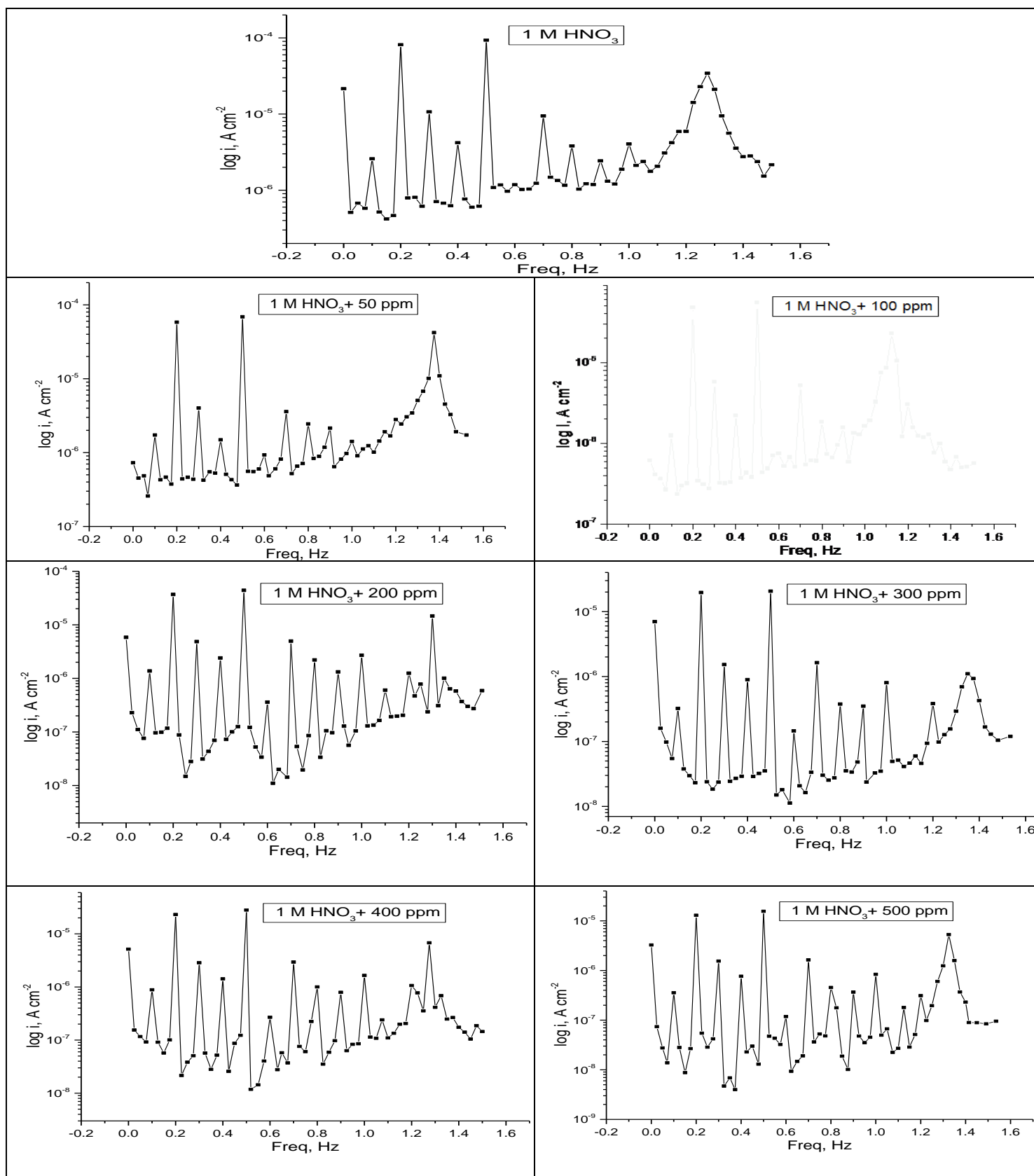
Figure 6. Intermodulation spectrum for Cu10Ni alloy in 1 M HNO$_3$ solutions without and with various concentrations of AUUE at 45°C.

Table 3. Electrochemical kinetic parameters obtained by EFM technique for Cu10Ni alloy in 1 M HNO$_3$ solutions containing various concentrations of AUUE at 25°C, 45C^o

Temp. °C	Concentration, ppm	i_{corr}, μA	β_a mV dec^{-1}	β_c mV dec^{-1}	C.R. mpy	CF-2	CF-3	θ	%IE
25	1 M HNO$_3$	62.7	49	76	28.67	2.44	2.20	---	---
	50	34.2	56	70	15.65	2.63	2.88	0.454	45.4
	100	30.4	53	80	13.88	2.86	2.66	0.516	51.6
	200	24.1	52	84	11.02	1.93	3.12	0.616	61.6
	300	17.2	76	119	7.88	1.86	3.09	0.725	72.5
	400	13.6	53	83	6.22	1.89	3.67	0.783	78.3
	500	8.5	62	108	3.88	1.99	2.48	0.865	86.5
45	1 M HNO$_3$	80.0	49	76	36.58	2.44	2.21	---	---
	50	60.5	56	70	27.63	2.62	1.88	0.244	24.4
	100	50.2	53	80	22.96	2.85	2.66	0.372	37.2
	200	39.7	52	84	18.16	1.93	2.23	0.503	50.3
	300	28.6	76	119	13.07	1.86	3.09	0.643	64.3
	400	25.4	53	83	11.60	1.89	3.64	0.683	68.3
	500	17.2	62	108	7.87	1.99	2.49	0.785	78.5

3.4. Adsorption isotherm

It is generally assumed that the adsorption of the inhibitors on the metal surface is essential step in the inhibition mechanism [33].
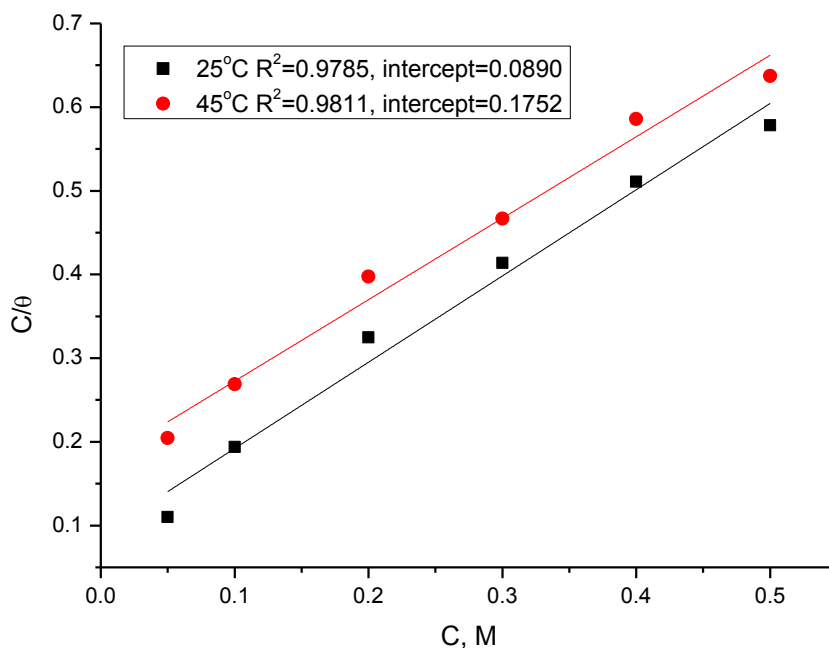

Figure 7. Curve fitting of corrosion data for Cu10Ni alloy in 1 M HNO$_3$ in the presence of different concentrations of AUUE to Langmuir adsorption isotherm at 25°C & 45°C.

To calculate the surface coverage (θ) it was assumed that the inhibitor efficiency (%IE) is due mainly to the blocking effect of the adsorbed species so (%IE = θ x100) [34]. In order to gain insight into the mode of adsorption of AUUE on Cu10Ni alloy surface, the surface coverage values from EFM technique were theoretically fitted into different adsorption isotherms and the values of correlation coefficient (R^2) were used to determine the best-fit isotherm. Figure (7) shows the plot (C/θ) vs. (C), which is typical of Langmuir adsorption isotherm at 25°C, and 45°C. Perfectly linear plot was obtained with regression constant (R^2) exceeding 0.9785 at 25°C and 0.9811 at 45°C and slope about unity. The deviation of the slope from unity, as observed from this study, could be interpreted to mean that there are interaction between adsorbate species on the alloy surface as well as changes in adsorption heat with increasing surface coverage [35, 36], factors that were ignored in the derivation of Langmuir isotherm.

The Langmuir isotherm is given by equation 7 [37]:

$$\frac{C}{\theta} = \frac{1}{K} + c \qquad (7)$$

where (C) is the inhibitor concentration and (K) is the equilibrium constant of adsorption process and is related to the standard free energy of adsorption ($\Delta G°_{ads}$) by equation 8:

$$k = \frac{1}{55.5} \, exp \left(\frac{-\Delta G°ads}{RT} \right) \qquad (8)$$

The value of (55.5) is the concentration of water in solution expressed in mole per liter, (R) the universal gas constant and (T) the absolute temperature. The calculated ($\Delta G°_{ads}$) values were also given in Table 4. The negative values of ($\Delta G°_{ads}$) ensure the spontaneity of the adsorption process and the stability of the adsorbed layer on the alloy surface [38]. It is well known that values of ($\Delta G°_{ads}$) of the order of -40 kJ mol^{-1} or higher involve charge sharing or transfer from the inhibitor molecules to metal surface to form coordinate type of bond(chemisorption); those of order of -20 kJ mol^{-1} or lower indicate a physisorption [39, 40]. The calculated ($\Delta G°_{ads}$) values (Table 4) were less negative than -20 kJ mol^{-1} indicate, therefore, that the adsorption mechanism of AUUE on Cu10Ni in 1 M HNO$_3$ solution is typical of physisorption. The lower negative values of ($\Delta G°_{ads}$) indicate that this inhibitor is not strongly adsorbed on the alloy surface.

Moreover, the adsorption heat can be calculated according to the Van't Hoff equation [41]:

$$\ln K = \frac{-\Delta H°_{ads}}{RT} + constant \qquad (9)$$

That is:

$$ln \left(\frac{K_2}{K_1} \right) = -\frac{\Delta H°_{ads}}{RT} \left(\frac{1}{T_2} - \frac{1}{T_1} \right) \qquad (10)$$

where ($\Delta H°_{ads}$) is the adsorption heat, (K_1) and (K_2) are the adsorptive equilibrium constants at T_1 (25˚C) and T_2 (45˚C), respectively. In consideration that the experiments precede at the standard pressure and the solution concentrations are not very high, which are close to the standard condition, the calculated adsorption heat thus can be approximately regarded as the standard adsorption heat

(ΔH°_{ads}) [41]. The negative values of (ΔH°_{ads}) (Table 4) reflect the exothermic behavior of the adsorption of AUUE on the Cu10Ni alloy surface.

Finally, the standard adsorption entropy (ΔS°_{ads}) can be calculated by the equation 11:

$$\Delta S^\circ_{ads} = \frac{\Delta H^\circ_{ads} - \Delta G^\circ_{ads}}{T} \qquad (11)$$

The (ΔS°_{ads}) values (Table 4) are positive, which are opposite to the usual expectation that the adsorption is an exothermic process and always accompanied by a decrease of entropy. The reason can be explained as follows: the adsorption of organic inhibitor molecules from the aqueous solution can be regarded as a quasi-substitution process between the organic compound in the aqueous phase [Org(sol)] and water molecules at the electrode surface [H_2O(ads)] [42]. In this situation, the adsorption of AUUE is accompanied by the desorption of water molecules from the electrode surface. Thus, while the adsorption process for the inhibitor is believed to be exothermic and associated with a decrease in entropy of the solute, the opposite is true for the solvent [43]. The thermodynamic values obtained are the algebraic sum of the adsorption of organic inhibitor molecules and the desorption of water molecules [44].Therefore, the gain in entropy is attributed to the increase in solvent entropy [43]. The positive values of (ΔS°_{ads}) suggest that the adsorption process is accompanied by an increase in entropy, which is the driving force for the adsorption of AUUE on the Cu10Ni alloy surface. Table 4 lists all the above calculated thermodynamic parameters.

Table 4. Equilibrium constant (K_{ads}) and adsorption free energy (ΔG°_{ads}) of AUUE adsorbed on Cu10Ni alloy surface in 1 M HNO_3 at 25˚C and 45˚C.

Temp., K	Langmuir adsorption isotherm			
	K_{ads}, $g^{-1}l$	$-\Delta G^\circ_{ads}$, kJ mol^{-1}	$-\Delta H^\circ_{ads}$, kJ mol^{-1}	ΔS°_{ads}, J K^{-1} mol^{-1}
298	11.24	15.95	26.69	36.04
318	5.71	14.27	26.69	39.05

3.5. Effect of temperature and activation parameters on inhibition process

The importance of temperature variation in corrosion study involving the use of inhibitors to determine the mode of inhibitor adsorption on the metal surface. Recently, the use of two temperatures to establish the mode of inhibitor adsorption on a metal surface has been reported and has been found to be adequate [45, 46]. Thus, the influence of temperature on the corrosion behavior of Cu10Ni alloy in 1 M HNO_3 in the absence and presence of AUUE of varying concentrations were investigated by EFM method at 25°C and 45°C. Therefore, in examining the effect of temperature on the corrosion process, the apparent activation energies (E_a) were calculated from the Arrhenius equation [47]:

$$\log\frac{k_2}{k_1} = \frac{E_a}{2.303R}\left(\frac{1}{T_1} - \frac{1}{T_2}\right) \qquad (12)$$

where (k_2) and (k_1) are the corrosion rates at temperature (T_1) and (T_2) respectively, and (R) the molar gas constant. An estimate of heat of adsorption was obtained from the trend of surface coverage with temperature as follows [48]:

$$Q_{ads} = 2.303R\left[\log\left(\frac{\theta_2}{1-\theta_2}\right) - \log\frac{\theta_1}{1-\theta_1}\right] \times \left(\frac{T_1 \times T_2}{T_2 - T_1}\right) \qquad (13)$$

where (θ_1) and (θ_2) are the degrees of surface coverage at temperatures (T_1) and (T_2), The calculated values for both parameters are given in Table 5.

Table 5. Calculated values of activation energy (E_a) and heat of adsorption (Q_{ads}) for Cu dissolution in 1 M HNO$_3$ in the absence and presence of AUUE at 25˚C and 45˚C

Conc., ppm,	E^*_a, kJ mol^{-1}	-Q_{ads}, kJ mol^{-1}
1 M HNO$_3$	9.59	--
50	22.40	37.21
100	19.83	23.09
200	19.69	18.02
300	19.92	15.08
400	24.55	20.34
500	27.85	22.07

Increased activation energy (E_a) in inhibited solutions compared to the blank suggests that the inhibitor is physically adsorbed on the corroding metal surface while either unchanged or lower (E_a) in the presence of inhibitor suggest physisorption mechanism [48]. It is seen from Table 5 that (E_a) values were higher in the presence of the AUUE compared to that in their absence hence leading to reduction in the corrosion rates. It has been suggested that adsorption of an organic inhibitor can affect the corrosion rate by either decreasing the available reaction area (geometric blocking effect) or by modifying the activation energy of the anodic or cathodic reactions occurring in the inhibitor-free surface in the course of the inhibited corrosion process [49]. The (E_a) values support the earlier proposed physisorption mechanism. Hence, corrosion inhibition is assumed to occur primarily through physical adsorption on the copper surface, giving rise to the deactivation of these surfaces to hydrogen atom recombination. Similar results have been reported in earlier publications [50].The negative (Q_{ads}) values indicate that the degree of surface coverage decreased with rise in temperature, supporting the earlier proposed physisorption mechanism [51].

3.6. SEM examination

In order to verify if the AUUE molecules are in fact adsorbed on Cu10Ni surface, SEM experiments were carried out. The SEM micrographs for Cu10Ni surface alone and after 24 h immersion in 1 M HNO$_3$ without and with the addition of 500 ppm of AUUE are shown in Figure (8).As expected, Figure (8a) shows metallic surface is clear, while in the absence of the AUUE, the Cu10Ni surface is damaged by HNO$_3$ corrosion (Figure (8b). In contrast, in presence of the AUUE (Figure 8c), the metallic surface seems to be almost no affected by corrosion, which suggest the adsorption of AUUE on the Cu10Ni alloy surface and confirm the formation of a thin film of AUUE observed in SEM micrograph, thus protecting the surface against corrosion.
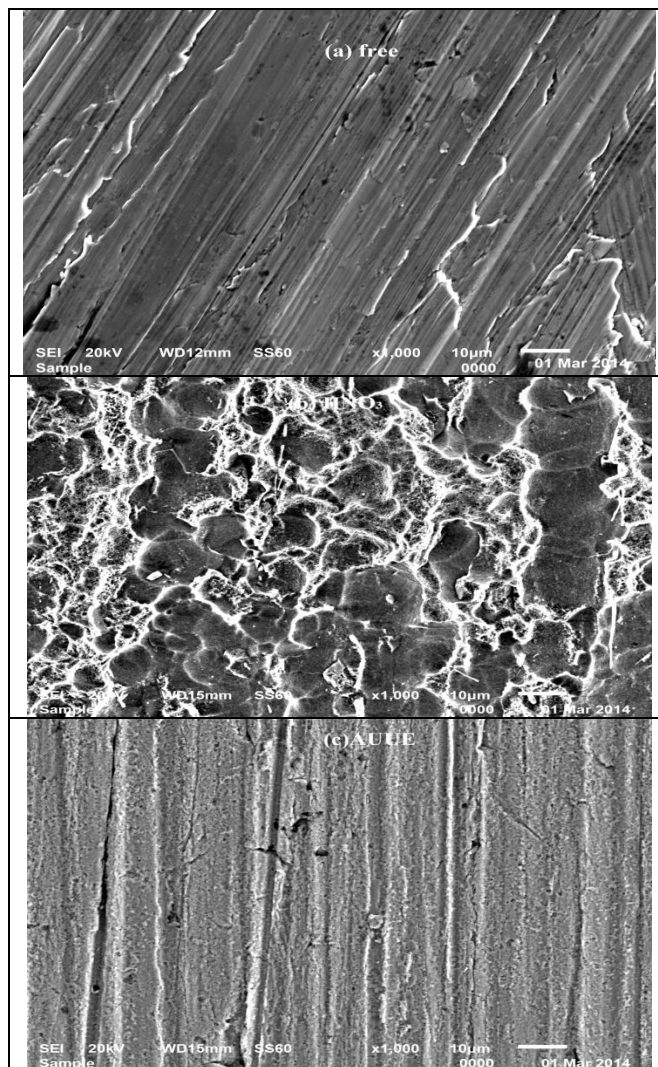
Figure 8. SEM micrographs of Cu10Ni surface (a) before of immersion in 1 M HNO$_3$, (b) after 24 h of immersion in 1 M HNO$_3$ and (c) after 24 h of immersion in 1 M HNO$_3$+ 500 ppm AUUE at 25°C

3.7. Mechanism of inhibition

Most organic inhibitors contain at least one polar group with an atom of nitrogen or sulphur or in some cases selenium and phosphorus. The inhibiting properties of many compounds are determined by the electron density at the reaction center [52].

With increase in electron density in the center, the chemisorption between the inhibitor and the metal are strengthened [53, 54]. The plant extract AUUE is composed of numerous naturally occurring organic compounds. Accordingly, the inhibitive action of AUUE could be attributed to the adsorption of its components on the Cu10Ni alloy surface. The constituents of AUUE are phytochemical constituents is arbutin, ursolic acid, tannic acid, gallic acid, some essential oil and resin, hydroquinones (mainly arbutin up to17%), tannins (up to 15%), phenolic glycosides and flavonoids [15]. Most of these phytochemicals are organic compounds that have center for π-electron and presence of hetero atoms such as oxygen and nitrogen; hence, the adsorption of the inhibitor on the

surface on Cu10Ni alloy is enhanced by their presence. The inhibition efficiency of methanol extracts of AUUE is due to the formation of multi-molecular layer of adsorption between alloy and some of these phytochemicals. Results of the present study have shown that AUUE inhibits the acid induced corrosion of Cu10Ni alloy by virtue of adsorption of its components onto the alloy surface. The inhibition process is a function of the metal, inhibitor concentration, and temperature as well as inhibitor adsorption abilities, which is so much dependent on the number of adsorption sites. The mode of adsorption was mixed one, chemisorption and physisorption observed could be attributed to the fact that AUUE contains many different chemical compounds, which some can be adsorbed chemically and others adsorbed physically. This observation may derive the fact that adsorbed organic molecules can influence the behaviour of electrochemical reactions involved in corrosion processes in several ways. The action of organic inhibitors depends on the type of interactions between the substance and the metallic surface. The interactions can bring about a change either in electrochemical mechanism or in the surface available for the processes [55].

4. CONCLUSIONS

From the overall experimental results the following conclusions can be deduced:

1. AUUE is good inhibitor and act as mixed type but mainly act as cathodic inhibitors for Cu10Ni alloy corrosion in 1 M HNO_3 solution.

2. The results obtained from all electrochemical measurements showed that the inhibiting action increases with the inhibitor concentration and decreases with the increasing in temperature.

3. Double layer capacitances decrease with respect to blank solution when the plant extract is added. This fact confirms the adsorption of plant extract molecules on the alloy surface.

4. The adsorption of inhibitor on alloy surface in 1 M HNO_3 solution follows Langmuir isotherm for AUUE extract.

5. The negative values of the free energy of adsorption and adsorption heat are indicate that the process was spontaneous and exothermic.

6. The values of inhibition efficiencies obtained from the different independent quantitative techniques used show the validity of the results.

References

1. G.Trabanelli, *Corrosion*, 47 (1991) 410.
2. A. K. Satapathy, G. Gunasekaran, S.C. Sahoo, K. Amit, R.V. Rodrigues, *Corros. Sci.,* 51 (2009) 2848.
3. V. V. Torres, R. S. Amado, C. F. De Sa, T. L. Fernandez, C. A. S. Riehl, A. G. Torres , E. D'Elia, *Corros. Sci.*, 53 (2011) 2385.
4. D. Gopi, K.M. Govindaraju, L. Kavitha, *J.Appl. Electrochem*, 40 (2010) 1349.
5. N. Patni, S. Agarwal, P. Shah, *Chinese J. Engineering*, (2013) doi.org/10.1155/2013/784186.
6. K.O. Orubite, N.C. Oforka, *Mater. Lett*., 58 (2004) 1768.
7. N. A. Negm, M. A. Yousef, S. M. Tewfik, *Recent Patents on Corrosion Science,* 3 (2013) 1.

8. M. Sangeetha, S. Rajendran, T.S. Muthumegala, A. Krishnaveni, *ZAŠTITA MATERIJALA,* 52 (2011) 3**.**
9. H. A. Al-Malki, M.Sc thesis, "A Study of Some Natural Products as Corrosion Inhibitors for Aluminium-Copper Alloy in Aqueous Media", Umm El-Qura University, Makah El-Mokarma (2007).
10. N. M. Al-Qasmi, M. Sc. Thesis, "Natural Products as Corrosion Inhibitors of Some Metals in Aqueous Media", Umm El-Qura University, Makah El-Mokarma (2010).
11. I. M. Mejeha, A. A. Uroh, K. B. Okeoma, G. M. Alozie, *African J. Pure and Applied Chem*., 4 (2010) 158.
12. M. Casebeer, Discover California Shrubs. Sonora, California: Hooker Press. ISBN 0-9665463-1-8 , (2004).
13. M. Grieve, (2007), http://www.botanical.com - A Modern Herbal.
14. K. A. Head, *Altern Med Rev.*, 13 (2008) 227.
15. P. B. Ronald, A. Rybarczyk, R. Amarowicz, *Polish Journal of Food and Nutrition Sciences,* 58 (2008) 485.
16. R. G. Parr, R. A. Donnelly, M. Levy, W. E. Palke, *J. Chem. Phys*., 68 (1978) 3801.
17. R. W. Bosch, J. Hubrecht, W. F. Bogaerts, B. C. Syrett, *Corrosion*, 57 (2001) 60.
18. L. Larabi, O. Benali, S. M. Mekelleche, Y. Harek, *Appl.Surf. Sci*., 253 (2006) 1371.
19. K. M. Ismail, *Electrochim. Acta*, 52 (2007) 7811.
20. T. I. Qin, J. Li, H. Q. Luo, M. Li, N. B. Li, *Corros. Sci*., 53 (2011) 1072.
21. T. Paskossy, *J. Electroanal. Chem*., 364 (1994) 111.
22. F. B. Growcock, J. H. Jasinski, *J. Electrochem. Soc*., 136 (1989) 2310.
23. S. S. Abd El-Rehim, K. F. Khaled, N. S. Abd El-Shafi, *Electrochim. Acta*, 51 (2006) 3269.
24. M. Metikos, R. Hukovic, Z. Bobic, S. Gwabac, *J. Appl. Elactrochem*., 24 (1994) 772.
25. A. Caprani, I. Epelboin, Ph. Morel, H. Takenouti, proceedings of the 4th European sym. on Corros. Inhibitors, (1975)571.
26. J. Bessone, C. Mayer, K. Tuttner, W. J. lorenz, *Electrochim. Acta*, 28 (1983) 171.
27. I. Epelboin, M. Keddam, H. Takenouti, *J. Appl. Electrochem*., 2 (1972) 71.
28. A.V. Benedeti, P.T.A. Sumodjo, K. Nobe, P.L. Cabot, W.G. Proud, *Electrochimica Acta,* 40 (1995) 2657.
29. H. Ma, S. Chen, L. Niu, S. Zhao, S. Li, D. Li, *Journal of Applied Electrochemistry* 32 (2002) 65.
30. X. H. Li, S. D. Deng, H. Fu, *J. Appl. Electrochem*., 40 (2010) 1641.
31. M. Lagrenee, B. Mernari, M. Bouanis, M. Traisnel, F. Bentiss, *Corros. Sci*., 44 (2002) 573.
32. S. S. Abdel-Rehim, K. F. Khaled, N. S. Abd-Elshafi, *Electrochim. Acta*, 51 (2006) 3269.
33. R.K. Dinnappa, S.M. Mayanna, *J. Appl. Electrochem*., 11 (1981) 111.
34. N. Patel, A. Rawat, S. Jauhari, G. Mehta, *European J. Chem.*, 1 (2010) 129.
35. J.I. Bhat, V.D.P. Alva, *J. Korean. Chem. Soc.*, 55 (2011) 835.
36. E.E. Oguzie, B.N. Okolue, E.E. Ebenso, G.M. Onuoha, A.I. Onuchukwu, *Mater. Chem. Phys*., 87 (2004) 394.
37. P.W. Atkins, *Physical Chemistry*, *6th Ed*., Oxford University Press, 1999; pp. 857- 861.
38. S.A. Umoren, U.F. Ekanem, *Chem. Eng. Comm*., 197 (2010) 1339.
39. K. Aramaki, N. Hackerman, *J. Electrochem. Soc*., 116 (1969) 568.
40. L. Tang, X. Li, L. Li, G. Mu, G. Liu, *Appl. Surface Sci*., 252 (2006) 6394.
41. T.P. Zhao, G.N. Mu, *Corros. sci.*, 41 (1999) 1937.
42. A. Döner, G. Kardas, *Corros. Sci*., 53 (2011) 4223.
43. B.G. Ateya, B.E. El-Anadouli, F.M. El-Nizamy, *Corros. Sci*., 24 (1984) 509.
44. X.H. Li, S.D. Deng, H. Fu, G.N. Mu, *Corros. Sci*., 52 (2010) 1167.
45. P.C. Okafor, M.E. Ikpi, I.E. Uwah, E.E. Ebenso, U.J. Ekpe, S.A. Umoren, *Corros. Sci*., 50 (2008) 2310.
46. Y. Ren, K. Luo, G. Zhang, X. Zhu, *Corros. Sci*., 50 (2008) 3147.

47. E.E. Oguzie, *Corros. Sci.*, 49 (2007) 1527.
48. A.S. Fouda, A.A. Al. Sarawy, E.E. El. Katori, *Desalination*, 201 (2006) 1.
49. S. Martinez, M. Matikos-Hukovic, *J. Appl. Electrochem*, 33 (2003) 1137.
50. F.H. Assaf, M. Abou-Krish, A.S. El-Shahawy, M.Th. Makhlouf, Hala Soudy, *Int. J. Electrochem. Sci.*, 2 (2007) 169.
51. S.A. Umoren, I.B. Obot, E.E. Ebenso, P.C. Okafor, O. Ogbobe, E.E. Oguzie, *Anti-Corros. Meth. Mater.*, 5 (2006) 277.
52. R. R. Anand, R. M. Hurd, N. Hackerman, *J. Electrochem. Soc.*, 112 (1965) 138 .
53. E. L. Cook, N. Hackerman, *J. Phys. Chem.*, 55 (1951) 549.
54. J. J. Bordeaux, N. Hackerman, *J. Phys. Chem.*, 61 (1957) 1323.
55. A. K. Singh, M. A. Quraishi, *Corros. Sci.*, 52 (2010) 1529.